Moroccan Journal of Chemistry
ISSN: 2351-812X
http://revues.imist.ma/?journal=morjchem&page=login
Taoufik & al. / Mor. J. Chem. 10 N°2 (2022) 362-374
DOI: https://doi.org/10.48317/IMIST.PRSM/morjchem-v10i2.29999

Atomic-scale compression and tensile investigations for crystalline Aluminum using EAM and MEAM potentials

***Meryem TAOUFIK*|[a*], *Hanae CHABBA* [b], *Abdrahim BARROUG* [a], *Ahmed JOUAITI* [a], *Driss DAFIR* [b]**

[a] *Sultan Moulay Slimane University, Faculty of Sciences and Techniques, Beni Mellal, Sustainable Development Laboratory, Campus Mghila, BP 523, 23000 Beni-Mellal, Morocco*

[b] *Sidi Mohmed Ben Abdellah University, Faculty of Sciences and Techniques, Energy Production & Sustainable Development Laboratory, Fez, Morocco*

* *Corresponding author: meryem04.taoufiki@gmail.com*

Received 05 Jan 2022
Revised 22 May 2022
Accepted 25 May 2022,

Abstract

Metals are hugely applied in manufacturing such as aerospace and automobile. The coherent role to understand the Aluminum material has extremely manifested in structural analysis at the atomic scale. This investigation paper provides a brief summary focused on the influence of the interatomic potentials categories in applied deformation. Based on atomistic simulations, the Embedded Atom Method (EAM) and the Modified Embedded Atom Method (MEAM) potentials are used to perform accurately the differences and similarities. The internal vectors involved in atomic configurations were depicted by features matrix and the mechanical properties were calculated using the linear fitting as an approach method. The implementation of (MD) simulations allows clarifying the occurred divergence using specific parameters in each compression and tensile deformations. The simulations results agree with experimental observations in FCC crystalline Al. The application of MEAM potential showed the raised compactness by calculations the interatomic distance, at initial state and after each numerical process of deformation in the first detection of atomic neighbors. The material act differently, and depict a disparity in particular regions. More attention is in the following paper.

Keywords: *Aluminum (Al), tensile, compression, MD simulation, MEAM & EAM potentials, mechanical properties, RDF, Linear fitting.*

1. Introduction

In structural material, Aluminum, exhibit a significant resource used in almost every sectors, it has played a critical role in recent advances of technology as a building material, widely used in different applications due to its behavior and ability to manufacturing, likewise, its perfects mechanical, electrical, physical and chemical properties[1]. It is important to have a fundamental understanding of the material in atomic levels, using different interatomic potentials [2]. Molecular dynamics (MD) simulation is one of the most tools, of high-speed technology in last few decades in different field especially in material science[3], [4]. It is widely used to predict the behavior from the small to the big scale of investigated material [5]. It helps to reply in many investigations such as the approach of deformation under a set of parameters, in order to assess the security and the strength against the failure, of different type of structure across the applied loads [6], [7]. From the major implementation of mechanical properties used is, the compression and the tensile deformation, the mechanism occurred by the variation of equilibrium state from the initial atomic position to the new atomic position, that explain the maximum failure in irreversible state. The computational simulation replies by strain-stress curves to obtain analysis of specific material [8]. Two types of behavior regions is presented, in the first, the material conserve it initial state and return to it after unapplied force, hence, the relationship between the principal parameters of deformation depict a Hoke's law [9], to calculate the slope of elasticity region. The second part is the plasticity, whereby the atomic bonds stretched, the dislocation and defaults are created and eventually stop the atomic movement. Our theoretical investigation in crystalline Al is based on one direction of deformation, the change of shape analysis under applied force illustrates the interactions between atoms and their evolutions, permit to examine various properties of the material, elastic constant, elasticity limit of the flexibility part. The uniaxial-tensile has the opposite of the internal interatomic force via the applied force, compared to uniaxial-compression behave in the same orientation of force from external to internal vectors [10]. The atomic crystal existing in nature are created via the electrostatic potential, generated from the Colombian forces between the particles of each atom, an extensive amount of research has been carried out of this kind. Hence, the atomic simulations required primordially the empirical interatomic potentials to describe the atomic behavior; the specific using influence the results. We performed the empirical potential MEAM and its original potential EAM, using the uniaxial-compression & uniaxial-tensile deformations of pure Al. Our study was mostly focused on a comparison of these two types of potential. Embedded Atoms Method (EAM), optimized for specific properties, including different metals with FCC crystal structure, H.N. Pishkenari et al. demonstrate the three independent elastic constant C_{11}, C_{12} and C_{44} for different FCC metals including the crystalline Al [11]. In parallel, Mendelev et al. [12] and M.I. Pascueta [13] work also on elasticity region under deformation using MEAM and EAM potentials respectively, in comparison, G.N. Kamm et al. [14] have been measured the elastic constant C_{44} using the ultrasonic pulse-echo technique in different low temperature, illustrate an agreement with simulation observation aforementioned. The current study carried out using the linear fitting analysis depict approximately the same range of previous results, in this regard, the calculation of interatomic distance is our goals under specific parameters, the results showed a short distance between Al atoms from initial state to final state. The atomic number generated about 30 000 atoms in the two different potentials at the same strain rate 1×1010 s-1, the temperature of 300K & 1 atmospheric pressure. The details analysis depicting radial distribution function (RDF), elasticity and plasticity predicting the linear fitting and the elastic constant C_{44} in each deformation type, all could figure out and enhance the interpretation of the material behavior. The investigation achieved with the helping smart tools to describe a visualized performance, the explanation detailed in the remaining paper.

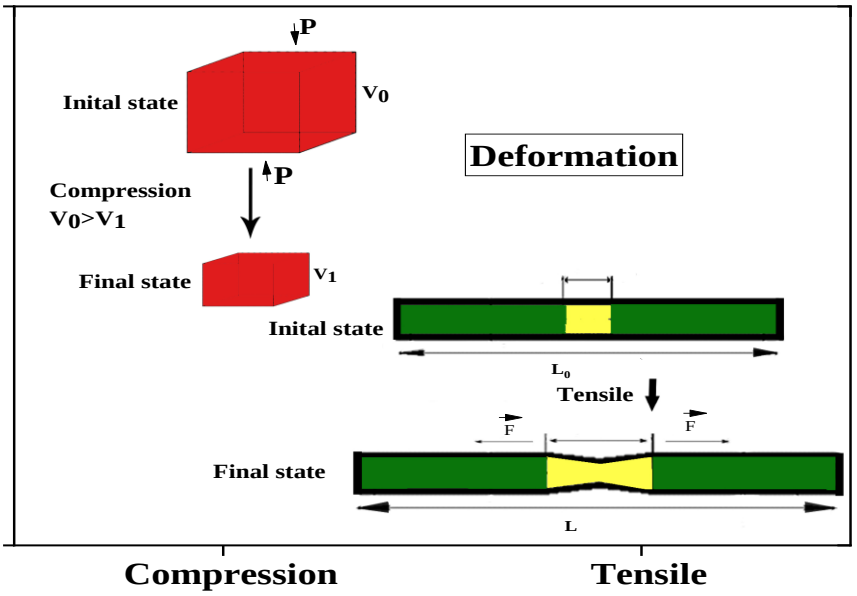

Figure 1. Principe of tensile & compression deformations

2. Materials and methods

2.1. Crystalline Aluminum

In crystallographic structure, atomic Al are arranged in face-centered cubic FCC, lattice parameter is 4.05 Å, the square angle is equal to α=β=γ=90° and space group belong to Fm-3mm at ambient temperature. The Table.1 shows the Al properties and was added such as parameters in numerical simulations [15], [16].

Table 1. Pure Al properties

Element	**$_{13}$Al**
Crystallographic Structure	FCC
Lattice parameter	a= 4.05
Space group	Fm-3m
Familly	Metal
Melting point	660°C
Electronic Configuration	[Ne]3s^2 3p^1

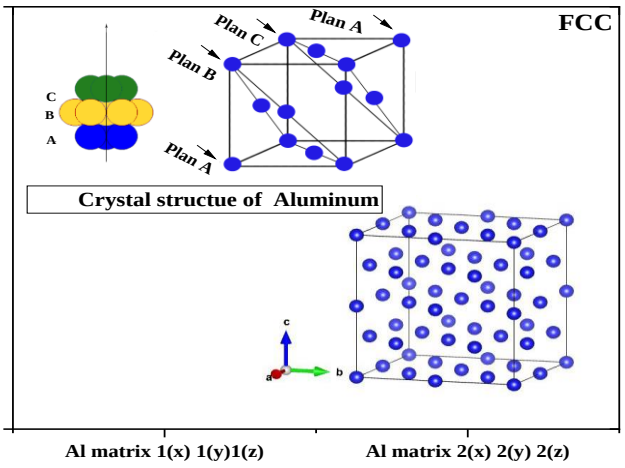

Figure 2. Unit cell structure & space lattice of pure crystalline Al.

The atomic structural of Al is crystalizing in FCC crystallography and have 4 atomic mesh, visualized at spread shape illustrate in fig.2 and the stacking recognize and configures with a layer sequence of following the ordered ABCABCABC… in the established matrix. The ratio between this two significant parameters is young's modulus also denote with letter E or elastic modulus C. Based on Voigt's notation, the hook's law can be written as:

$$[\sigma] = [c][\xi] \quad \& \quad [\xi] = [s][\sigma] \qquad (1)$$

The computational direction in x-, y-, and z-axes define the elastic constants as a linear part of strain-stress curves where $[\sigma]$ & $[\varepsilon]$ are 6x1 matrices, $[C]$ and $[S]$ are stiffness and compliance tensors; 6x6 square matrices that transform strains to stresses and vice versa. We applied Voigt notation the matrix of stiffness constants:

$$C = \begin{bmatrix} C_{11} & C_{12} & C_{13} & C_{14} & C_{15} & C_{16} \\ C_{21} & C_{22} & C_{23} & C_{24} & C_{25} & C_{26} \\ C_{31} & C_{32} & C_{33} & C_{34} & C_{35} & C_{36} \\ C_{41} & C_{42} & C_{43} & C_{44} & C_{45} & C_{46} \\ C_{51} & C_{52} & C_{53} & C_{45} & C_{55} & C_{56} \\ C_{61} & C_{62} & C_{63} & C_{64} & C_{65} & C_{66} \end{bmatrix} \qquad (2)$$

For the case of FCC metal, the opposite sides and the symmetry of the mesh are reduced and lead to only C_{11}, C_{12} & C_{44}. This investigation interested by a single C_{44} using two different potentials. Each element of the matrix [C] can be calculated as: $C_{ij} = C_{ji} = \frac{\partial u}{\partial \xi_i \partial \xi_j}$ (3)

2.2. The empirical interatomic potentials: EAM & MEAM

The first interatomic potential employed in this research was the EAM [17], used to describe a pair atomic behavior in the simulation system. It is one of the spread semi empirical interatomic potentials for metallic and their alloys, employed to describe the atomic interaction and calculate the energy of atoms in metallic structure. This potential has been used and validated in several MD simulations; the energy of system could be represented as [18]

$$E = \sum_{i=1}^{N} \left[F_i(\bar{\rho}_i) + \frac{1}{2} \sum_{j \neq i} \emptyset_{ij}(r_{ij}) \right] \qquad (4)$$

The second one, is the Modified Embedded Atom Method (MEAM) Potential [19], is one of the major and sufficient semi-empirical interatomic potentials. The structural material, elastic properties and the combinations of per elements are advanced to establish MEAM's parameters. In order to investigate the pure element or the alloying behaviors, the total system energy E of atoms calculated using an approximation in accordance with the form [20] $E = \sum_{i=1}^{N} \left[F(\bar{\rho}_i) + \frac{1}{2} \sum_{j \neq i} S_{ij} \emptyset(r_{ij}) \right]$ (5)

Where F_i is the embedding energy as the function of the average electron density $\bar{\rho}_i$ and $\emptyset_{ij}$ is the pair potential between atoms *i* and *j* separated by a distance r_{ij}, and S_{ij} is the screening factor ($0 \leq S_{ij} \leq 1$). The electron density of atom *i* is obtained from the sum of the electron density of the neighboring atom *j*. The electron density can be computed as: $\rho_{h,i} = \sum_{j \neq i} \rho_j^a(r_{ij})$ (6)

ρ_j^a is the electron density caused by atom j at distance r. Hence, the total electron density at each atom is the total sum of electron densities caused by other nearby atoms of structures. The first (MEAM) potential for silicon was affirmed to be capable to characterize and define all the building process, in the description for elasticity and defect properties containing surfaces energies. To illustrate a single crystalline Al using molecular dynamics, the (EAM) and the (MEAM) are employed to compare their interatomic behaviors between atomic pair elements Al-Al. The MEAM potential parameters are listed below for single pure Al: The reference structures for Al, crystallize in FCC. The cohesive energy is E_c, the equilibrium lattice parameter is a_0, A is the scaling factor for the embedding energy, α is the exponential decay factor for the universal energy, $\beta^{(0-3)}$ are the exponential decay factors for the atomic densities, $t^{(0-3)}$

are the weighting factors for the atomic densities, C_{max} and C_{min} are screening parameters, ρ_0 is the density scaling factor that is relevant only for element pairs[20].

Table 2. Sets of the MEAM potential parameters for single element Al

Parameters	Ec (eV)	a_0 (A)	A	α	$\beta^{(0)}$	$\beta^{(1)}$	$\beta^{(2)}$	$\beta^{(3)}$	$t^{(0)}$	$t^{(1)}$	$t^{(2)}$	$t^{(3)}$	C_{min}	C_{max}	ρ_0
$_{13}$Al	3.353	4.05	1.07	4.64	2.04	3.0	6.0	1.5	1.0	4.50	-2.30	8.01	0.8	2.8	1

3. Simulation details

Our MD simulations provide the atomistic properties and reveal the evolution characteristics of crystalline Al. To build the atomic model, firstly, the material's structure has been optimized, secondly, the periodic boundary conditions (PPP) are applied in x, y and z orientations, the simulation is elaborated in an Al matrix of 10(x)×10(y) ×10(z) FCC unit cells. The x, y, and z axes are respectively, along the [100], [010], and [001] crystallographic orientations. The box incorporate the atom numbers almost ~ 30000 particles, with a fixed time step Δt=1 fs, a temperature of 300K and an ambient atmospheric pressure. The lattice constant $a = b = c = 4.05$ Å and the interatomic potential are implemented in two cases: the EAM and the MEAM potentials are defined. In the simulation steps, Newton's second law is used to calculate the motions of atoms during the applied forces F(t) in a specific time t, for each mass m corresponding to atom i, we defined the force exerted by the whole system as follows [6].

$$a(t) = \frac{F(t)}{m} \quad (7)$$

$$F(t) = \nabla U(x(t), t) \quad (8)$$

Where a(t) is the atom's acceleration at the same time determined, x(t) is the atom's position at accurate time selected, U is the potential energy function. The equations of motion are employed, using Verlet Algorithm to solve it numerically [21], [22]. Each time step for integration of equation was 1 fs and all the simulations are performed with a micro-canonical NPT (isothermal-isobaric) ensemble i.e., constant number N of atoms at a constant pressure P and temperature T [12], [23], was chosen, using a Nose Hoover thermostat governed at constant temperature [24], with a dumping of 100 fs. Periodic boundary conditions applied in 3D to reach an equilibrium state, while the strain rate chosen was 1.0×10^{10} s^{-1}. All MD simulations are performed using LAMMPS code (Large-Scale Atomic/Molecular Massively Parallel Simulator). It was developed by Plimpton[25] at Sandia National Laboratories. Atomistic simulation using scientific visualization and analysis program (OVITO) [26] and VESTA [27] used as the 3-D snapshot visualization of our coding. The statistical program (ORIGIN) as a plotting software used to present the atomic analysis. The parameters details are summarized in Table 3.

Table 3. Detailed simulation parameters

Number of atoms	30 000
Time-step (fs)	1
Temperature (k)	300
Pressure (Pa)	Ambient atmospheric
Ensemble	NPT
Boundary Conditions	PPP
Interatomic Potential	EAM, MEAM
Strain rate (s^{-1})	1.0×10^{10}

The interatomic potential depict fundamental features in MD simulations to promote the correlation between atomic particles. The behavior during a uniaxial-compression and uniaxial-tensile illustrate different results & perform plastic straining.

4. Results and discussions

The crucial section depicts a similarity between EAM and MEAM interatomic potentials implementing the molecular dynamic simulations in order to characterize the behavior of crystalline Al, under the same concept of deformation. The theoretical investigation reproduces the atomic variation from the initial state to the final state, applying the uniaxial-compression and uniaxial-tensile. The 3-D snapshots for both technics have been visualized from datasets, and have been illustrated in figure 3.

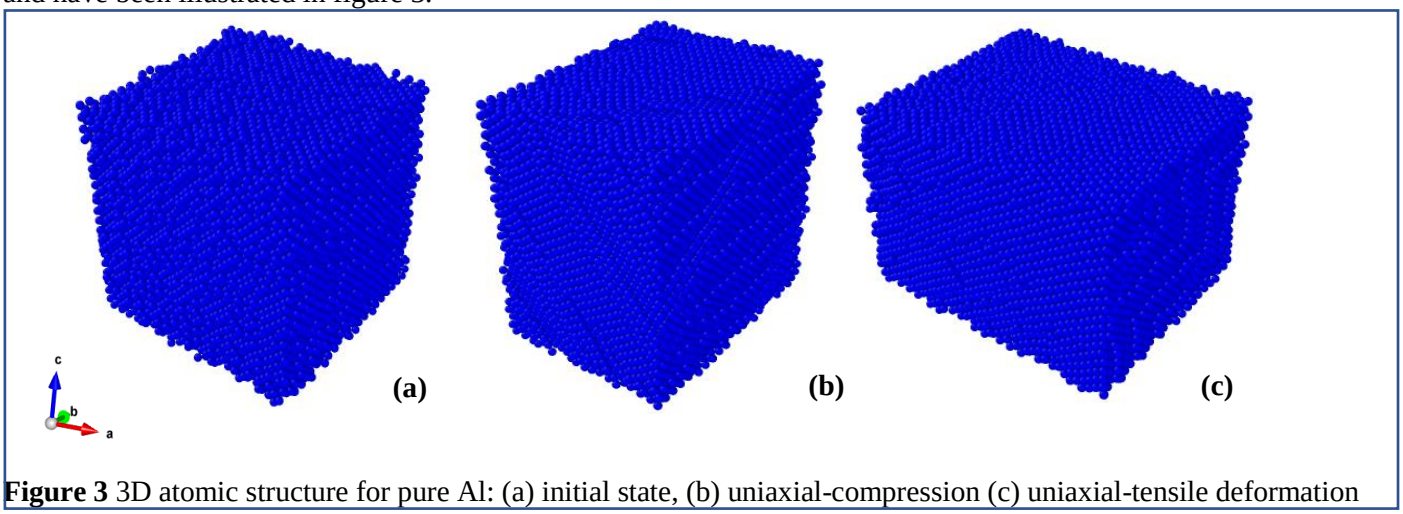

Figure 3 3D atomic structure for pure Al: (a) initial state, (b) uniaxial-compression (c) uniaxial-tensile deformation

The FCC elastic constants are the main factors manifesting the atomic behaviors for each used potential. We extracted C_{44} from matrix of compliance tensors as significant factors of rigidity, ductility, softness…etc. The presentation of uniaxial-tensile and uniaxial-compression applied in the provided interatomic potentials are depicted in figure 4.

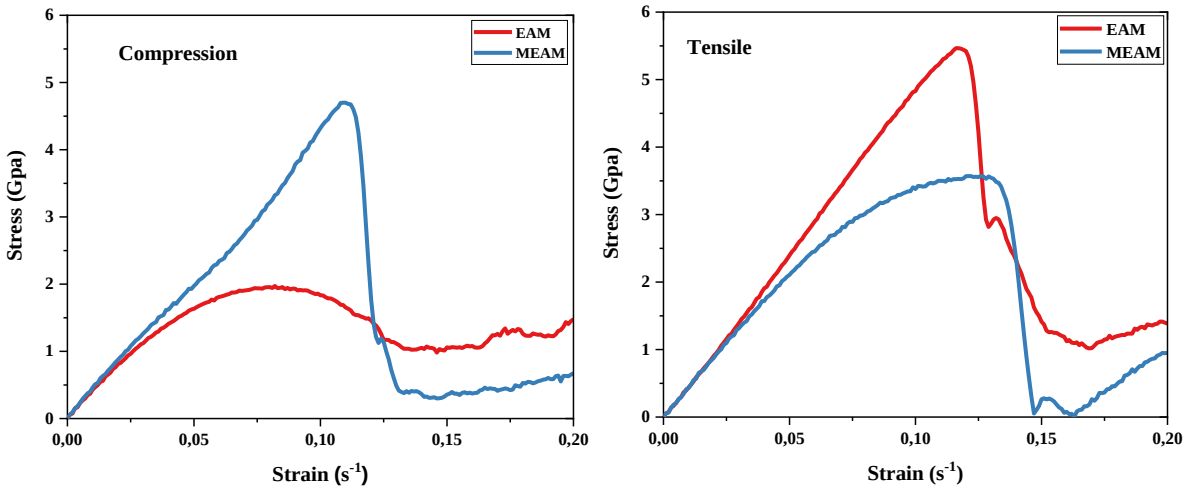

Figure 4. Stress-strain curves for crystalline Al under uniaxial-tensile and uniaxial-compression deformations

The line graphs depict the atomic behavior of crystalline Al under uniaxial straining using MEAM & EAM potentials at the strain rate $1.0\times10^{10}s^{-1}$. Overall, the technics emerge the same tendency of response; the atomic activity has reliance between its potential via the electrostatic of particles. The stress-strain curves

demonstrate that the atomic behavior under the external forces applied are different, and perform a fundamental part related to the linear region whereby the materials are malleable and reversible. The elastic constants of FCC Al metal arise, and the atomic bonds conserve its flexibility to return to their initial states after unapplied straining. The stress is linearly increased with strain and time steep. At the proportional limit of linear region, the materials eventually deviate from the point of departure of first region to the nonlinearity part called plasticity region, whereby, the Al atoms has been translated to the new equilibrium positions, their mobility can arise from dislocation motion. For uniaxial tensile, the EAM involves a long elasticity region of (5.4GPa /0.120s^{-1}) and the curve plummeted under a fracture of the metal, as important as MEAM potential, despite its reduced elasticity limit (2.5GPa / 0.0625s^{-1}) according to a special emphasis, depicted in a large plastic deformation. For uniaxial-Compression, using MEAM potential arise a significant elasticity limit (4.58GPa / 0.108s^{-1}) and a plummeting in plasticity region as a fracture, in contrast, the exploitation of EAM potential manifest a reduced elasticity region (1.41GPa/ 0.036s^{-1}) and a prominent plastic region. In simulation, the application of the empirical potential contribute in the variation of the behavior of same type of material investigated. Hence, the recognize of quantum effect become gradually meaningful. The crystalline structure affects the choice of empirical potential used, hence the atomic behavior of particles differs according to the mechanical description. Alternatively, the atomic configurations in y and z directions behave and fluctuate around zero. The behavior of σ_{yy} and σ_{zz} as a function of deformation ξ depicted in figure 5, the atomic velocities are correlated to the kinetic energy, hence the momentum represented by the atomic forces where the Newton second law are applied. The scalar field is the theory of potential energy, illustrate by the function of space and time. According to q(x,y,z) directions, in all the side surfaces the potential is constant, hence it referred to equipotential theory; the stress applied on the Al box introduce the atomic velocity of position, The gradient of the scalar field measures its rapidity. In order to compute the elastic constant for young and bulk modulus correlated to x-axe direction, the application of linear fitting is primordial. Regression coefficients are found for every potential used to specific technics of deformation. The underlying slope fitting technics implemented to estimate the properties of crystalline Al. The atomic diffusion in elastic region depends on its inertia via the atomic velocities. Its regression is represented in figure 6.

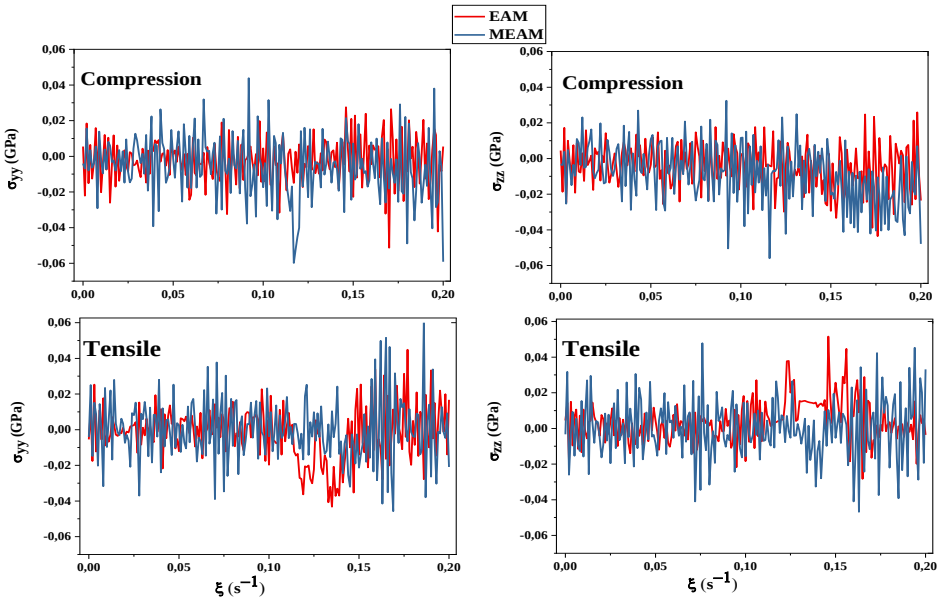

Figure 5. Stress-strain curves for crystalline Al applied along the y and z directions.

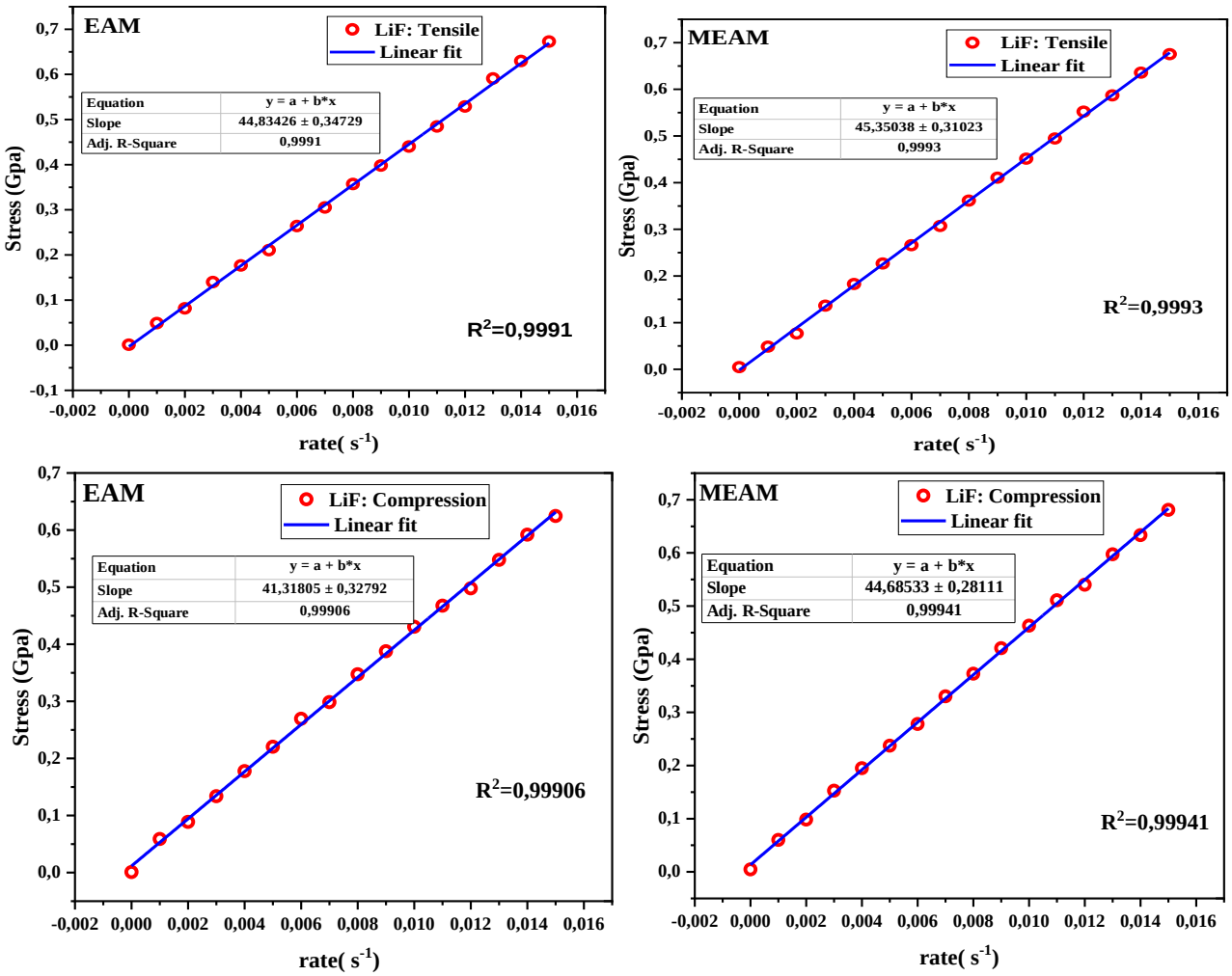

Figure 6. Elastic constant & coefficient of Pearson for crystalline Al under straining

The straight lines with a positive slope have a direction through all the given data. Hence, there is a very high agreement between linear fitting and the models fit of crystalline Al, in each mechanical deformations using EAM & MEAM potentials. The linear correlation coefficient of Pearson R^2 demonstrate this reliability, each result calculated is approximately ~1 (100%). The values provide a prediction of strong relationship between the stress & strain of deformation in the elasticity region. The only one factor impact the linear fitting of this investigation involve on resizing and reformatting the crystalline Al cells of the lattices under the activity of the external applied forces. The table 4 regroups the elastic constant C_{44} (GPa):

Table 3. the elastic constant C_{44} (GPa) using EAM & MEAM potentials

Potentials	Tensile	Compression	Previous study	Simulated	Experimental study	Literature	
Al^{EAM}	44.83	41.31	41[12]			35.25,	32.33
Al^{MEAM}	45.35	44.68	45.4 [13]		31.62 [14]	[15]	
$Error_{avg}$	0.33	0.305	0.22		-	-	

The computational elastic constant illustrates a harmony in the envisaged results. The comparison between theoretical and experimental studies depicts a tolerable accordance. Overall, the mechanical uniaxial-tensile illustrates a

significant increased elastic modulus in two applied potentials compared to uniaxial-compression. The interatomic distance using MEAM potential enhance and boost the hardness of crystalline Al from 44.83 to 45.35 & from 41.31 to 44.68 in uniaxial-tensile and uniaxial-compression methods respectively. The average errors have a compromise correlation.

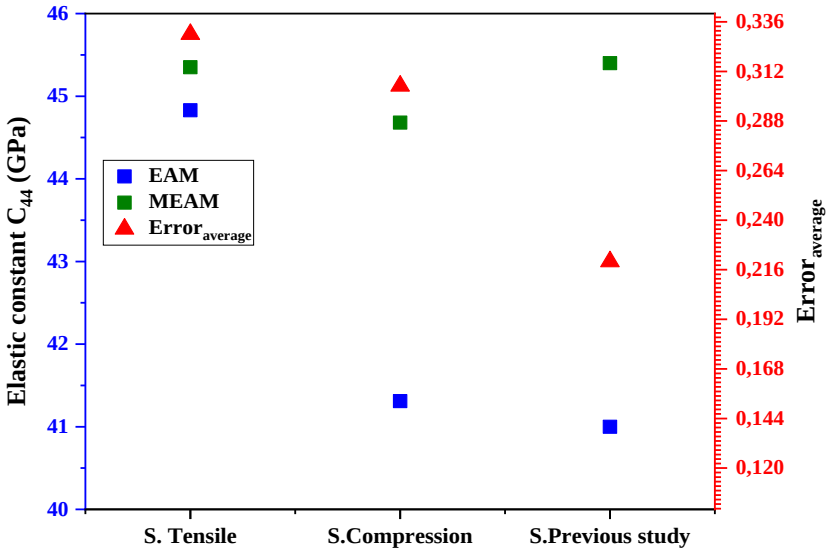

Figure 7. Current and previous investigation of elastic constant of deformation with error of pure Al.

In the same destination, the uniaxial-compression depict a decrease in yield strength, the end of process of deformation where the occurred fracture manifest also a decrease in the break point in both EAM and MEAM potentials. The special emphasis is devoted to emerge the uniaxial-tensile characterization in the support of the applied force on the material compared to the process of squeezes.

4.1. Radial Distribution Function (RDF)

The most intuitive way to operate the modeled atomic behavior via the bond length with the regards to the (MD) simulations is using the output datasets in analyzing the RDF tools. The behaviors are related to the probability of finding a particle for the first neighbors illustrated in the 1st shell and 2nd shell… until achieve no atomic correlations. The fluctuations describe the local order of crystalline Al. Hence, Figure 8 presents this characterization called radial distribution function RDF or g(r). It provides information about the probability of materials to calculate the bond length d between adjacent atoms. The general expression of RDF:

$$g(r) = \frac{1}{<\rho>} \frac{dn\,(r,dr)}{dv\,(r,dr)} \qquad (9)$$

Where dn is the number of atoms in a spherical shell, dv is a spherical shell volume, r is the distance of the shell from an arbitrary atom selected as the origin, $<\rho>$ is the average particle density.

To recognize the evolving changes occur between atoms, the exploitation of RDF is primordial, the probability of finding a particle in a specific position provide more details. The function behaves with proportionality under the neighbors around the central atomic of typical reference, the estimation of atomic bond $2R_0$ =d is related to the first maximum picks. The RDFs give good agreement to the following atomic attitude via the external applied forces.

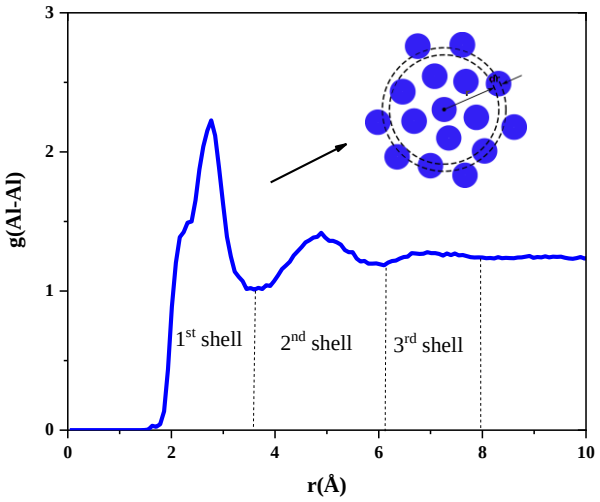

Figure 8. Allure of RDF descriptors and its atomic illustration

The fluctuate peaks indicate from initial to final states in the process of deformation, demonstrate a relation between the central particles of Al and nearest neighbors presented in the first shell, second sell, 3nd sell..etc until the correlations between atoms disappear. The simulation is carried out & illustrated in Fig.9. The investigation will provide more properties using EAM and MEAM potentials, the particular concepts of RDF descriptors are depicted us follow:

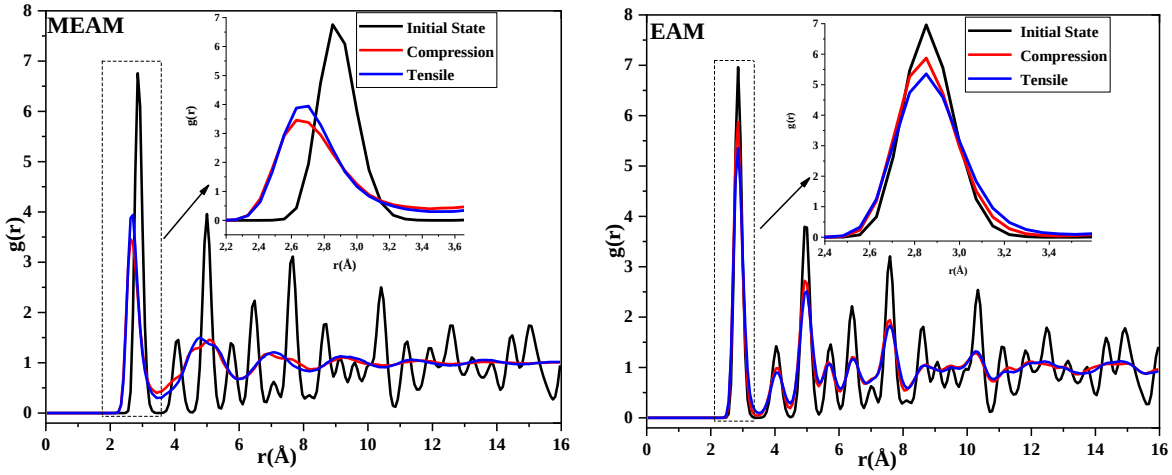

Figure 9. RDF using MEAM & EAM potentials via molecular dynamics (MD) simulation

At atomic scale, the diffuclties arise to recognize the system state with more precision, the probability of the presence of particles in space region is a significant factor to obtain more information about set of atoms. The RDF is a practical tool emphasis this approach. The function used permit to define the volumes $dv = dx.dy.dz$ around a typical particales of atom $M(x, y, z)$ where the probabilty of presence or finding an atoms is maximal.

Table 6. Interatomic distances & g(r) for the first neighbors for both potentials

	MEAM		**EAM**		**Literature**
	g(r)	**r(Å)**	**g(r)**	**r(Å)**	**r(Å)**
Initial State	6.7592	2.85185	6.96254	2.85185	3 [28], 2.86 [29]
Compression	3.45859	2.62963	5.87258	2.85185	3 [28]
Tensile	3.94276	2.7037	5.35679	2.85185	3.4 [19]

Overall, the potentials provide different output sets-data applied in RDF descriptors, the distinction potential from the original EAM to the modified MEAM facilitate the analysis and the comparison at atomic scale. The graphs illustrated in Figure 9 describe the RDF for crystalline Al and after both deformations using EAM and MEAM potentials. In the same trend, the curves have a change in the fluctuation and intensities, hence the position of peaks contribute various particularity and details in the local structure of the crystalline Al matrix. In addition, g(r) introduces numerous peaks, the firsts are very intensive compared to other peaks in all states. The utilization of EAM potential illustrate a large probability and the atomic bonding stimulate the same value after deformation compared with the utilization of MEAM potential, a small atomic-sets of finding atoms in each shell of RDF, and a reduced interatomic distance. After the 6^{th} shell the atomic detection loses the correlations between atoms, then, the atomic disorder emerges. In addition, the appropriate features obviously remarkable manifested with increasing the distance between the typical atomic references. The variations of peaks damped to g(r) = 0 in straining, the reason associated to the breaking correlation between atoms, whereby the compensation of electrons around each atoms are affected, hence their conductivities reduced.

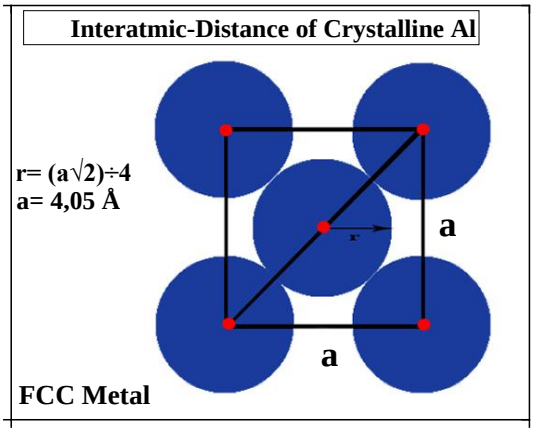

Figure 10. Calcul of lattice parametr of FCC crystalline metals on the face of the mesh

The outer layer of atomic crystalline Al has a low number of electrons, hence, the procol of whole atomic cohesion maintain the neutrality of crystal arises under atomic potential, since the atomic radius R_{Al}=1.43 Å gathered in prominence constant, the interatomic distance assuming to be different in each parameters of potentials used. The interatomic bonding illustrate the determinant factor based on electroic configuration $[Ne]3s^2\ 3p^1$, occuring the differences results between each potentials used, and represent the basis of crystallographic description of crystalline Al invistigated. The result of bonding using EAM and MEAM potential at initial state of homogeneous and ordered crystal structure depect in an ordered unit cells and uniform stoichiometric compositions of Al atoms. Results provided using MEAM potential define the shortest bonding compared to EAM potential, hence, the stronger atomic correlation and thus the mechanical strength incresed. Under the characterization of micro-canonical conditions, we calculated the variation of interatomic bonding, using MEAM potential ensure the shorter emcompassed interatomic bonding. The results are plotted in the figure 11. The bar chart provides information about variation of the interatomic distances Al-Al in the first neighbors of crystalline Al and their evolution under uniaxial-compression and uniaxial-tensile deformations in both EAM and MEAM potential. The interatomic MEAM Potentials used in each deformation confirmed the good atomic correlation by the short atomic bond, showed the raised compactness at initial state and after each numerical process of deformation proved and calculated at the first detection of atomic neighbors.

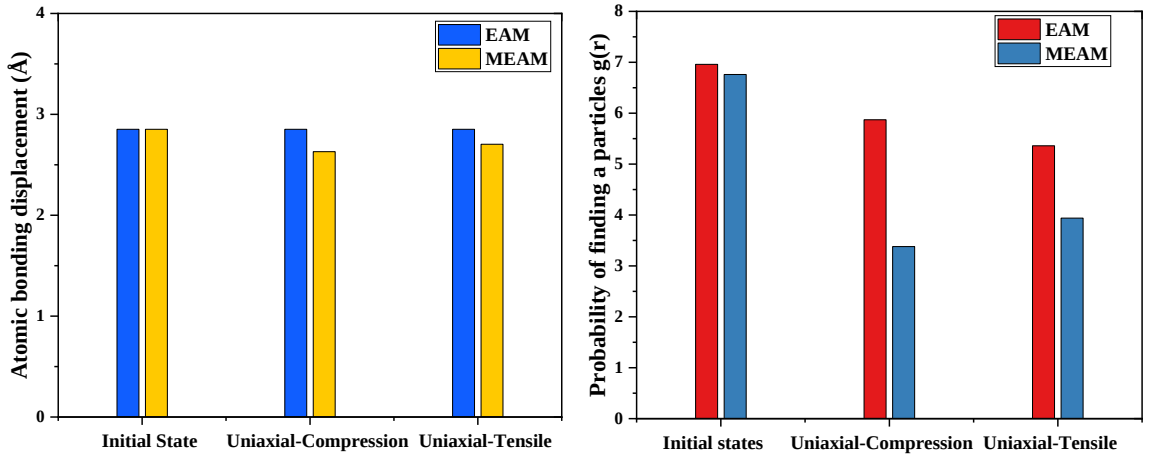

Figure 11. Initial interatomic distance and its evolution using EAM & MEAM potentials

Conclusion

The pure FCC Al is evaluated under the EAM and MEAM potentials using two types of deformations, tensile and compression, in order to define its mechanical properties. Following are the conclusions reached as a results of this simulation.

- methods used is molecular dynamics simulation of pristine Al to determine its the mechanical behavior and to arise the reliability with the experimental methods.
- Strain-Stress curves with the exploitations of EAM and MEAM potentials emerge different assessments in each type of deformation and that obviously reasonable by the shift of atomic configuration from a potential to another.
- Utilization of MEAM potential in order to calculate the elastic constant C_{44} of crystalline Al by using linear fitting demonstrate a convenient choice compared to employment of EAM potential with tensile concepts of deformation.
- The radial distribution function analysis of atomic behavior ensures the pervious results.
- The simulated and experimental results exhibit a good correlation.

References

[1] E. A. S. R.E., Jr. Sanders, P. Hollinshead, "Industrial development of non-heat treatable aluminum alloys.," *Mater. Forum*, no. 28, pp. 53-64., 2004.

[2] J. Jiang, P. Chen, and W. Sun, "Monitoring micro-structural evolution during aluminum sintering and understanding the sintering mechanism of aluminum nanoparticles: A molecular dynamics study," *J. Mater. Sci. Technol.*, vol. 57, pp. 92–100, 2020, doi: 10.1016/j.jmst.2020.03.068.

[3] D. C. Rapaport, *The Art of Molecular Dynamics Simulation*, Second edi. 2004.

[4] M. P. Allen & D. J. Tildesley, *Computer Simulation of Liquids*. New Tork, 1987.

[5] M. R. P. P. Dea, T. Frauenheim, *Computer Simulation of Materials at Atomic Level*, First edit. Berlin, 2000.

[6] B. S. D. Frenkel, *Understanding molecular dynamics simulation from algorithms to applications*, Second edi. London, 1996.

[7] D. Dong *et al.*, "Multiscale modeling of structure, transport and reactivity in alkaline fuel cell membranes: Combined coarse-grained, atomistic and reactive molecular dynamics simulations," *Polymers (Basel).*, vol. 10, no. 11, 2018, doi: 10.3390/polym10111289.

[8] M. A. Cooper, M. S. Oliver, D. C. Bufford, B. C. White, and J. B. Lechman, "Compression behavior of microcrystalline cellulose spheres: Single particle compression and confined bulk compression across regimes," *Powder Technol.*, vol. 374, pp. 10–21, 2020, doi: 10.1016/j.powtec.2020.06.089.

[9] T. Benitez, J. S. Rivas Murillo, D. de Ligny, N. Travitzky, A. P. Novaes de Oliveira, and D. Hotza, "Modeling the effect of the addition of alumina on structural characteristics and tensile deformation response of aluminosilicate glasses," *Ceram. Int.*, vol. 46, no. 13, pp. 21657–21666, 2020, doi: 10.1016/j.ceramint.2020.05.273.
[10] J.-P. A. I. and W. W. A. S. Krausz, J. I. Dickson, *constitutive laws of plastic deformation and fracture*, 19th ed. Ottawa: KLUWER ACADEMIC PUBLISHERS, 1989.
[11] A. Nejat Pishkenari, H., Yousefi, F. S., & TaghiBakhshi, "Determination of Surface Properties and Elastic Constants of FCC Metals: A Comparison among Different EAM Potentials in Thin Film and Bulk scale," *Mater. Res. Express.*, pp. 1–27, 2018, doi: doi:10.1088/2053-1591/aae49b.
[12] M. I. Mendelev *et al.*, "Development of interatomic potentials appropriate for simulation of devitrification of Al90Sm10 alloy," *Model. Simul. Mater. Sci. Eng.*, vol. 23, no. 4, p. 2015, 2015, doi: 10.1088/0965-0393/23/4/045013.
[13] M. I. Pascuet and J. R. Fernández, "SC," *J. Nucl. Mater.*, 2015, doi: 10.1016/j.jnucmat.2015.09.030.
[14] G. N. Kamm and G. A. Alers, "LowTemperature Elastic Moduli of Aluminum," vol. 327, no. May 2012, 1964, doi: 10.1063/1.1713309.
[15] L. R. F. J. Randolph Kissell, *Aluminum structures a guide to their specifications and design*, Second edi. New York, 1996.
[16] L. F. Mondolfo, *Aluminum Alloys Structures and Properties*. Butterworth, London, 1976.
[17] M. S. Daw and M. I. Baskes, "Embedded-atom method: Derivation and application to impurities, surfaces, and other defects in metals," *Phys. Rev. B*, vol. 29, no. 12, pp. 6443–6453, 1984, doi: 10.1103/PhysRevB.29.6443.
[18] M. S. D. S. M. Foiles, M. I. Baskes, "Embedded-atom-method functions for the fcc metals Cu, Ag, Au, Ni, Pd, Pt, and their alloys," *Phys. Rev. B*, vol. 33, pp. 7983–7991, 1986, doi: https://doi.org/10.1103/PhysRevB.33.7983.
[19] P. GANSTER, "Modelling of nuclear glasses by classical and ab initio molecular dynamics," MONPELLIER II, 2005.
[20] M. I. Baskes, "Modified embedded-atom potentials for cubic materials and impurities," *Phys. Rev. B*, vol. 46, no. 5, pp. 2727–2742, 1992.
[21] L. Verlet, "Comyuter 'Exyeriments' on Classical Fluids. I. Thermodynamical Properties of Lennard, -Jones Molecules~," *Phys. Rev.*, vol. 159, no. 1, pp. 98–103, 1967, doi: 10.1088/0022-3727/9/2/008.
[22] L. Verlet, "Computer 'Experiments' on Classical Fluids. II. Equilibrium Correlation Functions.," *Phys. Rev.*, vol. 165, no. 1, pp. 201–214, 1968, doi: 10.1103/PhysRev.165.201.
[23] S. Nosé, "A molecular dynamics method for simulations in the canonical ensemble," *Mol. Phys.*, vol. 52, no. 2, pp. 255–268, 1984.
[24] & V. F. J. Posch H. A., Hoover W. G., "Canonical dynamics of the Nosé oscillator: Stability, order, and chaos.," *Phys. Rev. A.*, vol. 33, no. 6, pp. 4253–4265, 1986.
[25] S. Plimpton, "Fast parallel algorithms for short-range molecular dynamics," *J. Comput. Phys.*, vol. 117, no. 1, pp. 1–19, 1995, doi: 10.1006/jcph.1995.1039.
[26] A. Stukowski, "Visualization and analysis of atomistic simulation data with OVITO-the Open Visualization Tool," *Model. Simul. Mater. Sci. Eng.*, vol. 18, no. 1, 2010, doi: 10.1088/0965-0393/18/1/015012.
[27] K. Momma and F. Izumi, "VESTA 3 for three-dimensional visualization of crystal, volumetric and morphology data," *J. Appl. Crystallogr.*, vol. 44, no. 6, pp. 1272–1276, 2011, doi: 10.1107/S0021889811038970.
[28] H. Chabba, M. Lemaalem, A. Derouiche, and D. Dafir, "Modeling aluminum using molecular dynamics simulation," *J. Mater. Environ. Sci.*, vol. 9, no. 1, pp. 93–99, 2018, doi: 10.26872/jmes.2018.9.1.11.
[29] F. R. S. H. J. Axon , D .P h il . and W. H ume-Rothery, "The lattice spacings of solid solutions of different elements in aluminium," *Proc. R. Soc. London. Ser. A. Math. Phys. Sci.*, vol. 193, no. 1032, pp. 1–24, 1948, doi: 10.1098/rspa.1948.0030.